terra digitalis
international e-journal of maps

Scientific geovisualization of the dynamics of sargassum dispersion and landfall in the Caribbean, based on satellite imagery and numerical forecasts ☆

Geovisualización Científica de la dinámica de dispersión y recale de sargazo en el Caribe, basada en imágenes satelitales y pronósticos numéricos

Francisco Javier Osorno-Covarrubias[a], Jorge Prado Molina[a], Gabriela Gómez[a], Uriel Mendoza[a], Stéphane Couturier[a,b]

[a]*Universidad Nacional Autónoma de México, Instituto de Geografía, Circuito Exterior s/n, Ciudad Universitaria, C.P. 04510, Ciudad de México, México.*
[b]*Integrative Crop Ecophysiology Group, Departament de Biología Evolutiva, Ecología i Ciéncies Ambientals, Facultat de Biología, Universitat de Barcelona, Avda. Diagonal, 643, CP 08028, Barcelona*

Abstract

This study focuses on the spatial and temporal representation of sargassum dispersal and landfall dynamics. An automated prototype is developed incorporating the following components: 1) Detection of sargassum rafts: Individual sargassum rafts are identified using Sentinel-2 images with a revisiting period of five days. 2) Forecasting/hindcasting vector fields: One-week forecasts (or hindcasts) are obtained at hourly intervals for the primary forces affecting raft movement—currents, tides, waves, and wind—using supercomputing services (Copernicus Marine Service) 3) Lagrangian simulation: The movement of rafts detected in step 1 is simulated using the vector fields obtained in step 2. For statistical purposes, rafts that land or drift outside the simulation range are logged with details of location, date, and time. 4) Animation generation: Four animations are produced to visualize: a) Rafts movement, b) Rafts trajectories, c) The dynamics of surface forcings (currents, tides, and waves), and d) The dynamics of above-surface factors (i.e. wind drag, modeled as a percentage of wind speed). 5) Interactive 3D visualization: All elements are integrated into an interactive globe featuring 3D bathymetry, allowing users to explore sargassum dispersion and landfall predictions (or hindcasts) for specific satellite observation dates. While the prototype shown takes into account all elements of a monitoring system, it should not be considered as an operational early warning system. In this study, we present the interactive geovisualization and discuss its potential for improving the scientific understanding of sargassum dispersal and landfall patterns, as well as its potential for the implementation of coastal management policies. A comparison is made with existing systems, highlighting the limitations and advantages of our approach while discussing its potential for developing a robust sargassum monitoring and early warning system for the Caribbean Sea.

Keywords: Dynamic 3D globe, geovisualization, dispersion and landfall dynamics, Sargassum monitoring, lagrangian marker, numerical forecasting

Resumen

Este estudio se enfoca en la representación espacial y temporal de la dinámica de dispersión y recale de sargazo. Para alcanzar este objetivo se desarrolla un prototipo de un sistema automatizado, que incorpora los siguientes elementos: 1) Detección de balsas de sargazo: Son identificadas balsas individuales de sargazo usando imágenes Sentinel-2 con un periodo de recurrencia de cinco días. 2) Obtención de pronósticos prospectivos/retrospectivos de campos vectoriales: los pronósticos o retrospectiva para una semana, se obtienen en intervalos de una hora para las principales forzantes que afectan el movimiento de las balsas (corrientes, mareas, oleaje y viento) usando servicios de supercómputo (Servicio Marino de Copernicus). 3) Simulación lagrangiana: El movimiento de las balsas individuales, detectadas en el paso 1, es simulado usando los campos vectoriales obtenidos en el paso 2. Para propósitos estadísticos los detalles de localización, fecha y hora de las balsas que recalan o derivan fuera del intervalo de simulación; son almacenados. 4) Generación de animaciones: Cuatro animaciones son producidas para visualizar: a) El movimiento de las balsas b) Sus trayectorias de movimiento, c) La dinámica de las forzantes superficiales (corrientes, mareas y oleaje), y d) La dinámica de los factores que actúan sobre la superficie (i.e. arrastre del viento, modelado como un porcentaje de su velocidad). 5) Visualización 3D: todos los elementos anteriores se integran en un globo interactivo con batimetría 3D, que permite a los usuarios examinar el pronóstico (prospectivo o retrospectivo) de dispersión y recale para una fecha específica del paso del satélite. Si bien nuestro prototipo conjunta todos los elementos relevantes de un sistema de monitoreo, no debe considerarse como un sistema operacional de alerta temprana. Aquí nos concentramos solamente en la geovisualización interactiva de la dinámica de los procesos de dispersión y recale y su significado para mejorar la comprensión científica, así como la implementación de políticas de gestión costera. Se compara nuestro sistema con otros similares propuestos y existentes. Se discuten las limitaciones y perspectivas de nuestro enfoque, así como su potencial para desarrollar un sistema robusto de monitoreo y alerta de sargazo para el mar Caribe.

Palabras clave: globo 3D dinámico, geovisualización, dinámica de dispersión y recale, monitoreo de sargazo, marcador lagrangiano, pronósticos numéricos

1. Introduction

1.1. Contextualizing the problem

Pelagic sargassum (*sargassum spp.*) is native to a region of the North Atlantic, between 20° and 40° North latitude and 80° to 20° West longitude, commonly known as the Sargasso Sea. This name derives from the distinctive appearance sargassum gives to these marine landscapes. However, the phenomenon of seasonal sargassum beaching originates from a new pelagic population in an area stretching from West Africa to the Gulf of Mexico, known as the Great Atlantic sargassum Belt (GASB) (Wang et al., 2019).

The retrospective analysis by Johns (Johns et al., 2020), based on numerical simulations of wind, currents, and satellite imagery, traces its origin to an extreme episode of the North Atlantic Oscillation (NAO) that occurred in the winter of 2009–2010; unusually strong and southwest-shifted westerly winds, along with the North Equatorial Current (NEC), pushed masses of sargassum from the tropical Atlantic to the northern equatorial recirculation zone. This, combined with the abundance of nutrients resulting from deforestation in the Amazon, Orinoco, and Magdalena River basins, triggered a "tipping point" in the biosphere that caused changes in ecosystems on an oceanic scale (figure 1. See also "Origin of GASB" in the interactive globe). From 2011 onwards, part of the biomass of this new Sargasso Sea, is transported from the coasts of the Equatorial Atlantic and Brazil, to the Caribbean, carried by the Guiana and Caribbean Currents. This transport is further reinforced by the northern trade winds, which blow consistently westward throughout the year.

Since 2011, the coasts of the Caribbean have experienced sargassum beaching events of varying intensity. In the western Caribbean, extreme accumulations of sargassum can occur at any time of the year, with increased frequency and coverage during the summer. Uribe-Martinez and collaborators reported historical peaks between July and October 2018 and from January to February 2019 (Uribe-Martinez et al., 2022).

Intense sargassum episodes have significant negative ecological impacts (Rodriguez-Martinez et al., 2019), and economic consequences (Schling et al., 2022). When sargassum washes ashore, it forms dense mats on the water's surface, altering light conditions and negatively affecting corals and benthic flora (Van Tussenbroek et al., 2017). Two to three days after stranding, sargassum begins to decompose, producing particulate matter and leachate that consume dissolved oxygen, resulting in the formation of a brown tide. On beaches, decomposing sargassum accumulates into foul-smelling heaps, often exceeding the removal capacity of both private and public entities (Figure 2).
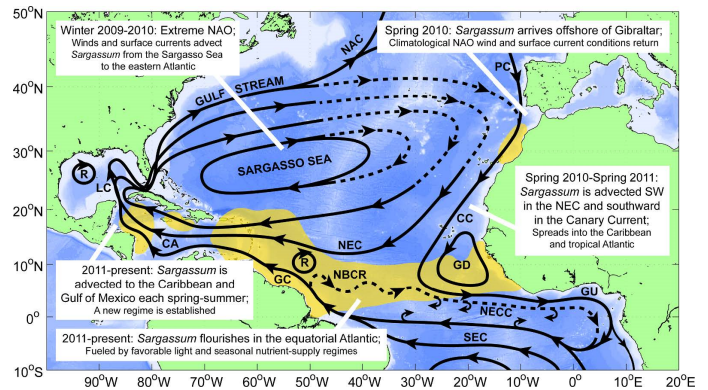
Figure 1. Model of the Great Atlantic Sargassum Belt (GASB). The new GASB is suspected to originate from an extreme episode of the negative phase of the North Atlantic Oscillation, during the winter of 2009-2010 (Figure taken from Jhons et al. 2020) / Figura 1. Explicación esquemática del origen del Gran Cinturón de Sargazo del Atlantico (GASB, por sus siglas en ingles) a partir de un episodio extremo de la fase negativa de la oscilación del Atlántico Norte, durante el invierno 2009-2010 (Figura tomada de Jhons et al 2020)

The removal of these masses is expensive and often inadequate. This process necessitates heavy equipment and sand raking operations that result in beach erosion. The collected decomposing biomass is transported to landfills, where leachates infiltrate the karst soil, contaminating the aquifers with organic residues and arsenic that living sargassum concentrates due to bioaccumulation processes (Olguin-Maciel et al., 2022).

A number of alternative uses have been evaluated to transform the adversity of massive sargassum beaching episodes into resources such as fertilizer, inputs for the pharmaceutical industry, livestock feed, and biofuel, among others (Chávez et al., 2020; Oxenford et al., 2021; Robledo et al., 2021). So far, the results are limited. The levels of toxins like arsenic and other heavy metals above acceptable thresholds make it non-viable as feed or fertilizer. Following commercial criteria it is challenging to identify and implement processes and products that are industrially competitive. Seasonal availability, variable, and unpredictable volume, limit its implementation (Milledge et al., 2020; Milledge & Harvey, 2016; Nielsen et al., 2021). Effective coastal management requires estimating in advance the volume, date, and approximate location of sargassum landings. This would allow anticipating the required resources, facilitating budgeting, procurement, redirect and optimize field crews and necessary equipment (Park et al., 2015).

1.2. Sargassum remote sensing

Pelagic sargassum drifts in the ocean, forming rafts that aggregate into thin streaks that can stretch for kilometers. To detect its position and estimate its volume on a regional scale (across the Caribbean), medium-resolution satellite images (500-1000m nominal) have commonly been used, employing the Floating Algae Index (FAI) or the Alternative Floating Algae Index (AFAI) (Wang & Hu, 2016). For example, the Optical Oceanography Laboratory at the University of

Figure 2. Sargassum accumulation on the beach, Playa del Carmen, QRoo, Mexico. May 31, 2021. / Figura 2. Acumulación de sargaso en Playa del Carmen, QRoo, Mexico, 31 de mayo de 2021.

South Florida (Hu et al., 2024) uses moderate-resolution images (MODIS, NASA) to examine the red edge reflectance (enhanced reflectance in the near-infrared) of floating vegetation, using both FAI and AFAI for the sargassum Watch System (SaWS). At more local scales, the indices can be extracted from the Multispectral Instrument (MSI) on the Sentinel-2 satellite operated by the European Space Agency (ESA), which has a spatial resolution of 20m. The revisit period of Sentinel-2 is 5 days, which does not allow the capture of rapid changes in its distribution.

1.3. Role of sargassum passive transport simulation

A key technique for understanding the dynamics of sargassum dispersal and landfall is the simulation of passive transport using forecasts (or hindcasts) of the relevant forces. Putman and collaborators conducted numerical experiments with synthetic particles to simulate the transport of sargassum from the equatorial Atlantic to the Caribbean Sea (Putman et al, 2018). The agreement of their results with historical data derived from satellite observations was fundamental in establishing the equatorial origin of the sargassum observed in the massive beaching events in the Caribbean, starting in 2011. In a experimental study with synthetic particles and oceanographic drifters Putman and collaborators (Putman, 2023) found that including a 1 to 3% windage factor reduced the separation distances between synthetic particles and the footprints of sargassum mats, pseudo sargassum drifts, and non-submerged oceanographic drifts.

The integration of remote sensing and passive transport simulation techniques enables the development of advanced monitoring and early warning systems. A notable precursor in this field is the SAMTool system (Collecte Localisation Satellites (CLS), 2023), created by the risk mitigation company "CLS Group" and supported by the ESA. This system combines six sensors operating in the visible, infrared, and radar spectrums to detect sargassum at a spatial resolution of 20 meters. It also provides trajectory forecasts for detected rafts using established current and wind models. However, its results are not publicly

accessible, as the service is subscription-based, and its algorithms are proprietary. A key objective of our research is to enhance accessibility by disseminating forecasts (or hindcasts) via an interactive web globe featuring dynamic animations.

In this article, we present an automated prototype system that includes the following processes: 1) detecting individual sargassum rafts using Sentinel-2 images, 2) obtaining forecasts (or hindcasts, for retrospective studies) of key forcings—currents, waves, tides, and wind—from supercomputing services, 3) simulating the movement of sargassum to forecast (or hindcast) raft trajectories and the timing of sargassum wash-ups, and 4) visualizing the results through a dynamic, interactive web map. Furthermore, we compare the functionality and communicative potential of our web mapping tool with existing online systems designed for monitoring and early warning of sargassum inundations.

2. Materials and methods

2.1. Study area

The study area corresponds to the region of the Mexican Caribbean, primarily covering the states of Quintana Roo, as well as the coasts of Guatemala, Belize, and part of Honduras (Figure 3). Specifically, 18 quadrants of the Sentinel-2 image grid are considered. Each quadrant is approximately 110 km wide by 110 km tall, which amounts to an area of about 12,060 km^2. Considering the overlaps between the images, the total study area is approximately 150,000 km^2.
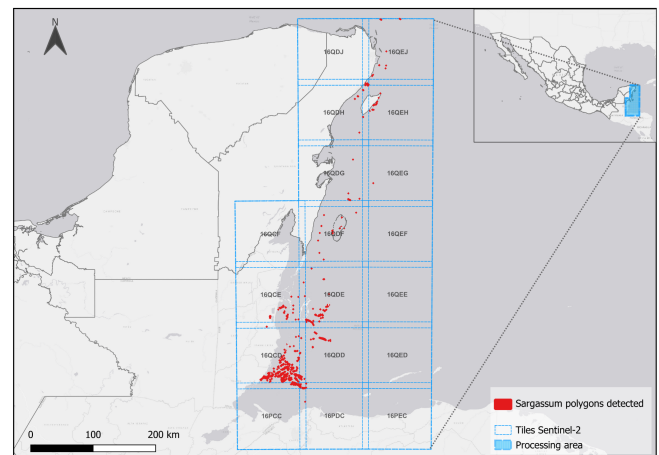

Figure 3. The western Caribbean Sea (includes the coasts of Mexico, Belize, Guatemala and part of Honduras). The footprint of the Sentinel-2 scenes used for sargassum detection appears in blue contours. Numerical forecast vector fields and passive transport simulations are cut off to this area. Red polygons show the location of sargassum rafts detected in June 4th, 2024 at 4:08 pm. / Figura 3. Caribe Continental (incluye las costas de México, Belize, Guatemala y parate de Honduras). Los contornos azules indican la huella de las imágenes Sentinel-2 usadas en la teledetección. Los pronósticos numéricos de las forzantes y las simulaciones de transporte pasivo se cortan a esta area. Los polígonos rojos muestran la ubicación de balsas de sargazo detectadas en las escenas del 4 de junio de 2024 a las 4:08 pm.

2.2. Detection of sargassum rafts with Sentinel-2

The "Sentinelsat" module is utilized through an API to automate the download of Sentinel images (Level 1 processing: L1) for the study area from the Copernicus Open Access Hub (Sentinelsat, 2023). Atmospheric correction is then applied using the Sen2Cor 2.12 package, which converts these images to surface reflectance (Level 2 processing: L2). Sargassum detection is then performed by analyzing the values of bands 4, 8, 8A, and 11, applying threshold conditions to the band values as follows: (b8A<0.07) and (b04<0.1) and (b11<0.05) and (b04<b8A) and (b04<b08). Where:

- b4 → 665 nm red band;

- b8 → 848 nm infrared band;

- b8A → 865 nm infrared band;

- b11 → 1610 nm shortwave infrared band.

Sargassum detection is filtered in transition zones between scenes using entropy filters. The results are then vectorized, and polygons which fall within the continental mass and those too close to clouds identified by the scene classification maps (SCL), are disregarded. Additionally, polygons with centroids located less than 100 meters from the coast are removed. An overview of the sargassum raft detection and extraction process is illustrated in a workflow diagram (Figure 4).
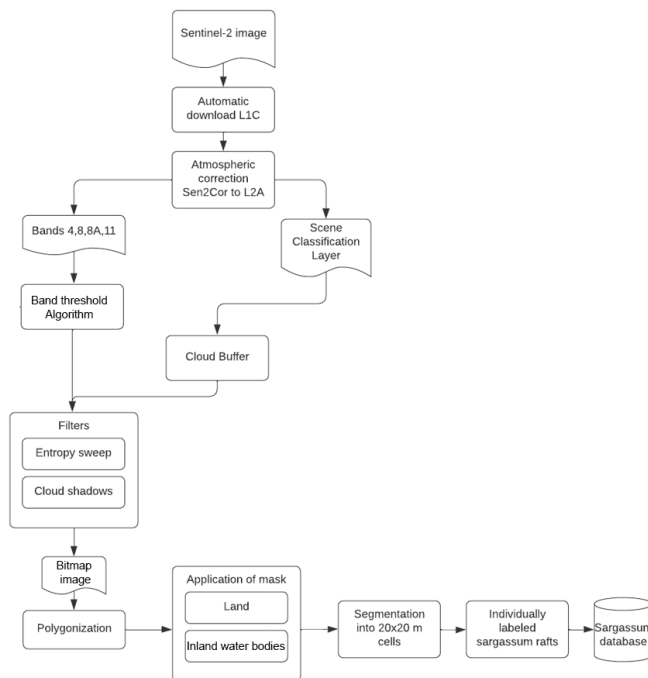

Figure 4. Workflow diagram for the detection and extraction of individual sargassum rafts and associated database / Figura 4. Diagrama de flujo para la detección y extracción de balsas individuales de sargazo y base de datos asociada.

The result of the above process is a set of traceable individual points, each of which establishes the initial position of sargassum rafts of the size of 20x20m cells. Each cell is thereafter floated through a vector field resulting from the sum of relevant forcings (following section).

2.3. Modeling passive transport of sargassum rafts

Sargassum rafts are primarily driven by surface currents, tides, wave action, wind friction, and the effect of ocean floor topography on currents.

Lagrangian and Eulerian approaches represent two distinct methods for studying fluid motion, each offering a different perspective on fluid behavior. The Lagrangian approach focuses on individual particles, tracking their trajectories, velocities, and accelerations. This method provides a microscopic view of fluid motion and is particularly useful for analyzing phenomena involving particle interactions and transport. In contrast, the Eulerian approach examines fixed points in the fluid, monitoring changes in fluid properties at those locations over time. While the Lagrangian approach calculates the trajectory of each individual particle, the Eulerian method concentrates on the overall concentration of particles, assessing the diffusion and convection of groups of particles. (Bible et al., 2020).

In our geovisualization prototype, marker tracking employs a Lagrangian approach, where the next position of each particle is determined based on its current location within the Eulerian grid of vector fields acting upon it. For the date and time of the satellite pass, we obtain the forecast/hindcast of the relevant variables from two separate data sets: the first one accounts for the immediate subsurface forcings (0.5 m depth), which includes current speed, tides and waves; the second one accounts for surface drag caused by wind, which is calculated as a fraction of the wind velocity at 10 m height. Both data sets are provided by the Copernicus Marine Service. Both simulations have a temporal resolution of one hour. The spatial resolution is 1/12° for the first and 1/8° for the second (Figure 5, A and B). Python code was developed to calculate the trajectory of sargassum rafts during the interval between two consecutive Sentinel images. Regarding the relevance of wind in passive transport, Putman et al. (2020) found that incorporating a windage factor of 1% to 3% reduced the separation distances between synthetic particles and the footprints of sargassum mats, pseudo-sargassum drifts, and non-submerged oceanographic drifters.

Finally, an online interactive map with forecasted trajectories was created (see section bellow).

3. Results

3.1. Dynamics of sargassum dispersion

A snapshot of our dynamic map (Figure 6A) shows the forecast of dispersion and beaching of sargassum detected in Sentinel images during the period from May 20th to 30th, 2024. Our forecast for this period was that 83% of the detected rafts would wash up.

Within the span of one day, drifting sargassum rafts can move up to 200 km with bursts of up to 3 m/s (10.8 km/h). During this time, they may reach the coast or move away quickly,
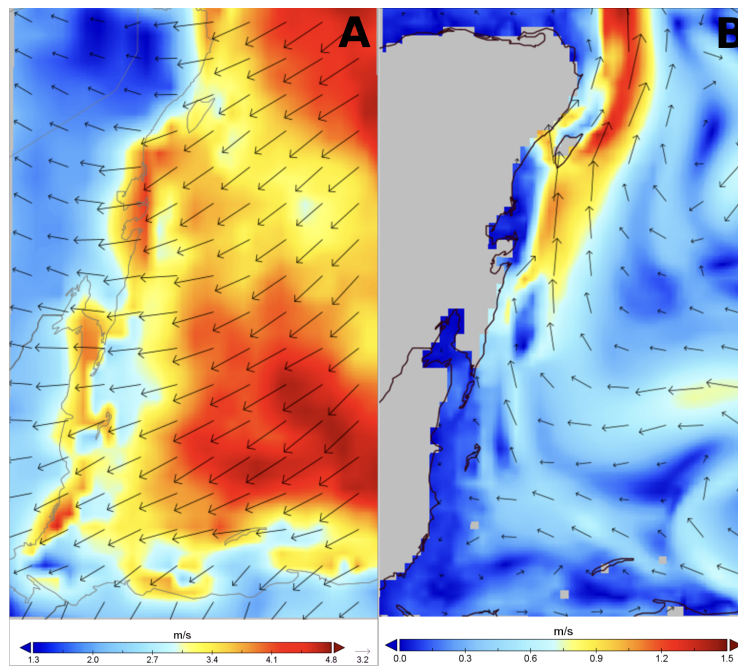
Figure 5A. Snapshot of the wind speed forecast at 10 m from the surface (May 20th, 2024 at 4:00 pm). Figure 5B. Snapshot of the forecast of the subsurface forcings (May 20th, 2024 at 4:00 pm). We considered the sum of the speeds of the currents, waves and tides at 0.5 m below the surface. / Figura 5A. Pronóstico de la velocidad del viento a 10 m de la superficie (20 de mayo de 2024 a las 4:00 pm). Figura 5B. Pronóstico de la velocidad de las forzantes inmediatamente abajo de la superficie (20 de mayo de 2024 a las 4:00 pm) Utilizamos la suma de velocidades de las corrientes, las mareas y el oleaje a 0.5 metros de la superficie.

travel along the shore, or rotate in irregular vortices whose center shifts slowly. Therefore, the amount of sargassum near a particular stretch of coast is not a good indicator of the amount that will wash up there.

At regional scale, the trajectories in the Gulf of Honduras show more complexity (figure 6B). In contrast with the linear trajectories off the Mexican coast (left side of the image), we found paths with loop patterns further away (on the lower right edge), which correspond to eddies and low-speed looping currents.

While our system has the characteristics of a monitoring and early warning system, it should not be used as an operational decision making tool. Its proper implementation requires further research and developments, including the improvement of the remote sensing technique, a more robust Lagrangian approach for passive transport simulation and an experimental protocole for accuracy assessment.

3.2. Comparison of our prototype with existing sargassum monitoring systems

The spatial resolution of our remote sensing input (20m) surpasses the one used in monitoring systems such as Florida's sargassum Watch System (SaWS) (Hu et al., 2024) (500m) and the sargassum Early Advisory System (SEAS) for the Texas coasts (30m) (Webster & Linton, 2013). It is comparable to the spatial resolution of the SAMTool system (Collecte Localisation Satellites (CLS), 2023), but our platform is open access and free of charge. The trajectories forecasted by our model reach

the coasts, unlike the SaWS system which has a buffer of 50 km offshore from the coastline. Both the prediction of beaching and the quantification of sargassum are facilitated by our model. Our visualization follows the principle of particle tracking (Lagrangian simulation), similar to NASA visualizers developed by Shirah and Mitchell (Sahirh & Mitchell, 2015), making the animation of simulated dispersion and beaching highly understandable by coastal management actors, compared to other animations available in online monitoring systems. Among all the systems mentioned, our system would be closest to the SAM-Tool or the sargassum Surveillance Bulletin for Guadeloupe (DEAL de Guadeloupe (Direction de l'Environnement & Meteo France, 2023).

However, there are several limitations to our prototype. To begin with, a validation with ground data has not yet been implemented. The revisit period for sargassum detection is much longer (5 days) than that of SaWS (12 hours). For the purpose of our system prototype, a sargassum detection algorithm based on threshold values has been used. With this approach, small sargassum rafts are generally not detected, but the intention was to minimize false positives, due to bright non-algal targets (including cloud artifacts and wave-induced glints) that highly reflect in the near-infrared spectrum, as described by Wang and Hu (2020). More precise sargassum detection is possible but much more computer intensive (Wang and Hu, 2021). In our study, the coarse space scale of the forcing fields is better adapted to the simulated path of large sargassum rafts. In terms of sargassum detection, options explored include com-
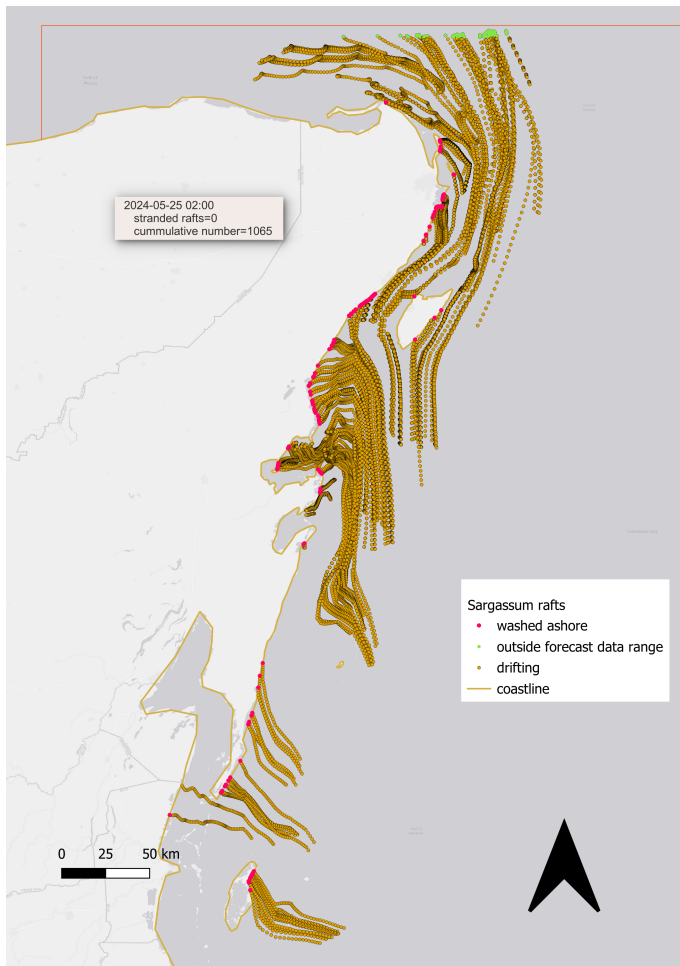
Figure 6A. Trajectories of the Sargassum rafts as simulated in this study. The Lagrangian simulation of individual rafts are tracked over a period of approximately five days (detection date: May 20th, 2024 at 4:00 pm, until May 25th at 2:00 am). Rafts are colored brown as they drift, red when they land, green when they leave the simulation data range. The dynamic label in the upper left corner shows the timestamp, the number of rafts making landfall and the total cumulative number up to the current timestamp (updated at hourly intervals) / Figura 6A. Trayectoria pronosticada de las balsas de Sargazo según nuesra simulación numérica. Se muestra la simulacion Lagrangiana de trayectorias de las balsas individuales durante un periodo de 5 días aproximadamente (fecha de detección 20 de mayo de 2024 a las 4:00 pm hasta el 25 de mayo a las 2:00 am). Coloreamos las balsas de cafe mientras flotan a la deriva, de rojo cuando recalan y de verde cuando salen del rango de datos de la simulación. La etiqueta dinámica en la esquina superior izquierda muestra la fecha y hora, el número y número acumulado, de balsas que recalan en durante y hasta, el intervalo en curso (intervalos de una hora)

bining Sentinel-2 images with lower resolution and higher frequency images, as in the case of the above-mentioned systems, to solve for cloud presence during the acquisition of Sentinel-2 images. The applicability of radar images should also be explored.

3.3. Dynamic web map

As the reliability of the forecast system gains robustness, the dynamic geovisualization we propose (Figure 7) has fea-

tures with promising perspectives in three aspects. 1) The visualization of trajectories can facilitate the intuitive understanding of sargassum dispersal and washout, allowing the authorities to anticipate volumes, areas and timeframes of sargassum landfalls; 2) The high quality near-real time visualizations could serve as an effective communication tool between operational response teams, the general public and local actors, in the process of preparing mitigation operations and obtaining the required resources; 3) As a consequence, it has the potential of increasing the efficiency of prevention measures and response tasks.

Additionally, the geovisualization in a Globe with 3D bathymetry opens perspectives for the analysis and communication of the underlying hydrodynamic models at the regional scale.

Finally, from a geoscience teaching perspective, the visual metaphor of a dynamic globe serves as an effective tool to illustrate the connectivity between global and local processes. This is exemplified by the regime shift at the ocean-basin scale, which has caused severe local impacts. The establishment of the new sargassum belt, driven by global environmental changes, demonstrates how large-scale phenomena can result in difficult-to-reverse local consequences.
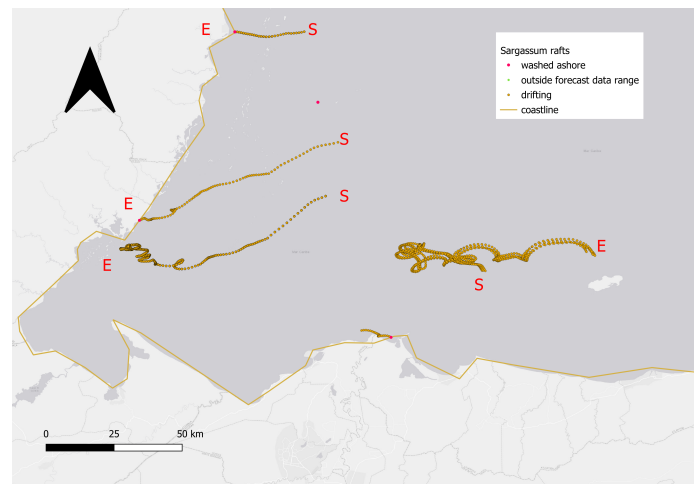

Figure 6B. Trajectories of Sargassum rafts at regional scale. Simulation from June 4th at 4:00 pm, to June 14th at 4:00pm (10 days). I: Initial position at satellite pass; F: final position. / Figura 6B. Trayectorias de las balsas de Sargassum a escala regional. Simulación desde el 4 de junio a las 4:00 pm hasta el 14 de junio a las 4:00 pm (10 días). I: Posición inicial en el paso del satélite; F: Posición final.
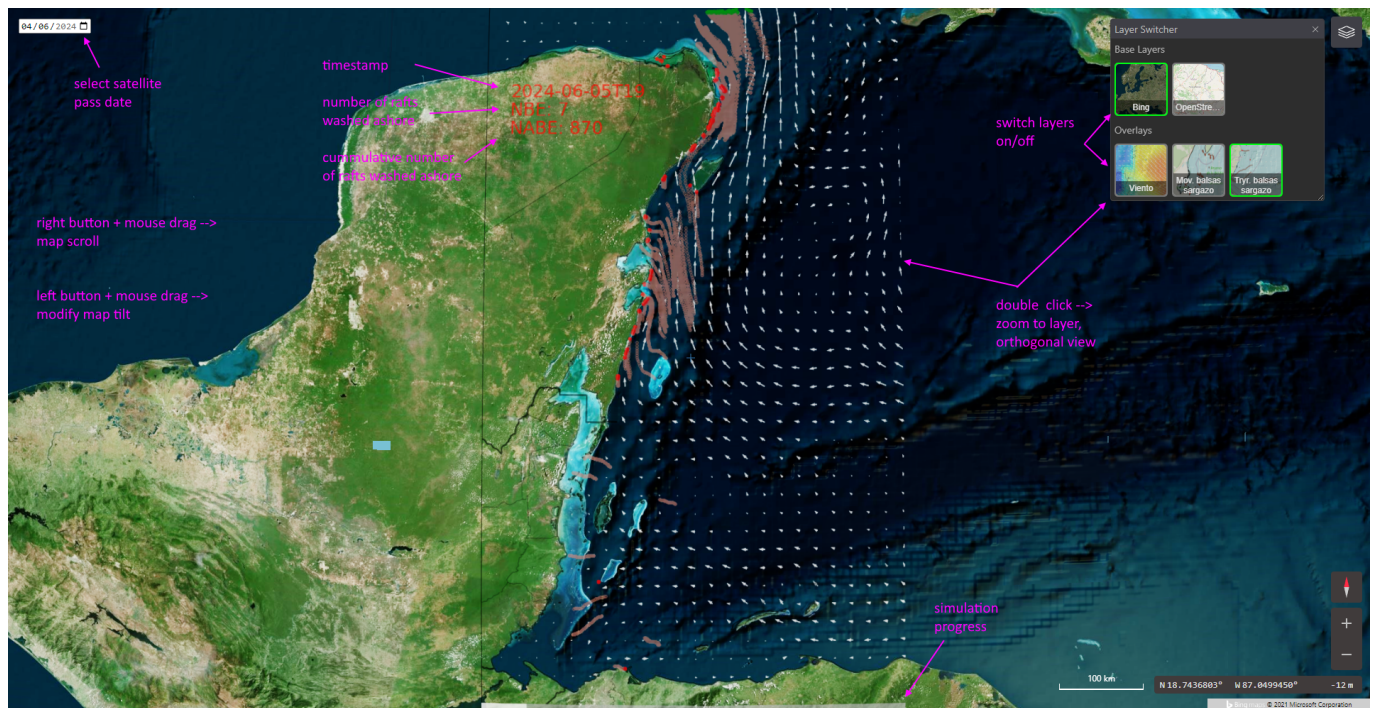
Acknowledgments and funding

Figure 7. Dynamic web globe. 1) Sentinel-2 pass date selector 2) Layer switcher: allows to switch between layers of sargassum movement, sargassum trajectories, and forecasted forcings (currents, tides, waves or wind). / Figura 7. Globo web dinámico. 1) Selector de fecha de paso del satelite Sentinel-2, 2) Control de capas: permite seleccionar alternar la capa activa: movimiento de las balsas, trayectorias, pronóstico de las forzantes subsuperficie (corrientes, mareas y oleaje) y sobre la superficie (viento).

References

Bible, S., Triece, C., Ryan, S., 2020. Navigating fluid motion: Lagrangian vs. Eulerian frames of fluid motion. Resolved Analytics, available at: https://www.resolvedanalytics.com/cfd-physics-models/lagrangian-vs-eulerian-phase-models [Accessed 15 Dec. 2024].

Chávez, V., Uribe-Martínez, A., Cuevas, E., Rodríguez-Martínez, R., van Tussenbroek, B., Francisco, V., Estévez, M., Celis, L., Monroy-Velázquez, L., Leal-Bautista, R., 2020. Massive influx of pelagic *Sargassum spp.* on the coasts of the mexican caribbean 2014–2020: challenges and opportunities. Water 12 (10), 2908, https://doi.org/10.3390/w12102908.

(CLS), C. L. S., April 2023. Samtool: Sargassum detection. En: Product documentation. Collecte Localisation Satellites, available at: https://datastore.cls.fr/products/samtool-sargassum-detection/ [Accessed 15 Dec. 2024].

DEAL de Guadeloupe (Direction de l'Environnement, d. l. e. d. L., France, M., April 2023. Prévision des échouages. En: Product documentation. Direction de l'Environnement, available at: https://www.guadeloupe.developpement-durable.gouv.fr/prevision-des-echouages-r1256.html [Accessed 15 Dec. 2024].

Hu, C., Barnes, B., Canizzaro, J., 2024. Satellite-based Sargassum Watch System (SaWS). Optical Oceanography Laboratory, College of Marine Science, University of South Florida, available at: https://optics.marine.usf.edu/projects/saws_test.html [Accessed 15 Dec. 2024].

Johns, E. M., Lumpkin, R., Putman, N. F., Smith, R. H., Muller-Karger, F. E., Rueda-Roa, D. T., Hu, C., Wang, M., Brooks, M. T., Gramer, L. J., 2020. The establishment of a pelagic sargassum population in the tropical atlantic: biological consequences of a basin-scale long distance dispersal event. Progress in Oceanography 182, 102269, https://doi.org/10.1016/j.pocean.2018.06.009.

Milledge, J. J., Harvey, P. J., 2016. Golden tides: Problem or golden opportunity? the valorisation of *Sargassum* from beach inundations. Journal of Marine Science and Engineering 4 (3), 60, https://doi.org/10.3390/jmse4030060.

Milledge, J. J., Maneein, S., López, E. A., Bartlett, D., 2020. *Sargassum* inundations in turks and caicos: Methane potential and proximate, ultimate, lipid, amino acid, metal and metalloid analyses. Energies 13 (6), 1523, https://doi.org/10.3390/en13061523.

Nielsen, B. V., Milledge, J. J., Hertler, H., Maneein, S., Al Farid, M. M., Bartlett, D., 2021. Chemical characterisation of *Sargassum* inundation from the turks and caicos: Seasonal and post stranding changes. Phycology 1 (2), 11, https://doi.org/10.3390/phycology1020011.

Olguin-Maciel, E., Leal-Bautista, R. M., Alzate-Gaviria, L., Domínguez-Maldonado, J., Tapia-Tussell, R., 2022. Environmental impact of sargassum spp. landings: an evaluation of leachate released from natural decomposition at mexican caribbean coast. Environmental Science and Pollution Research 29 (60), 91071–91080, https://doi.org/10.1007/s11356-022-22451-3.

Oxenford, H. A., Cox, S.-A., van Tussenbroek, B. I., Desrochers, A., 2021. Challenges of turning the sargassum crisis into gold: current constraints and implications for the caribbean. Phycology 1 (1), 27–48, https://doi.org/10.1080/017088.2021.1234567.

Park, K., Kaiser, K., Broman, B., 2015. SEAS Forecasting (SARGASSUM EARLY ADVISORY SYSTEM). SEAS Forecast, available at: http://seas-forecast.com/ [Accessed 15 Dec. 2024].

Putman, N. F., Beyea, R. T., Iporac, L. A. R., Triñanes, J., Ackerman, E. G., Olascoaga, M. J., Appendini, C. M., Arriaga, J., Collado-Vides, L., Lumpkin, R., Hu, C., Goni, G., 2023. Improving satellite monitoring of coastal inundations of pelagic sargassum algae with wind and citizen science data. Aquatic Botany 188, 103672, https://doi.org/10.1016/j.aquabot.2023.103672.

Putman, N. F., Goni, G. J., Gramer, L. J., Hu, C., Johns, E. M., Trinanes, J., Wang, M., 2018. Simulating transport pathways of pelagic sargassum from the equatorial atlantic into the caribbean sea. Progress in Oceanography 165, 200–209, https://doi.org/10.1016/j.pocean.2018.06.009.

Robledo, D., Vázquez-Delfín, E., Freile-Pelegrín, Y., Vásquez-Elizondo, R. M., Qui-Minet, Z. N., Salazar-Garibay, A., 2021. Challenges and opportunities in relation to sargassum events along the caribbean sea. Frontiers in Marine Science 8, 699664, https://doi.org/10.3389/fmars.2021.699664.

Rodríguez-Martínez, R. E., Medina-Valmaseda, A.-E., Blanchon, P., Monroy-Velázquez, L. V., Almazán-Becerril, A., Delgado-Pech, B., Vásquez-Yeomans, L., Francisco, V., García-Rivas, M. C., 2019. Faunal mortality associated with massive beaching and decomposition of pelagic sargassum. Marine Pollution Bulletin 146, 201–205, https://doi.org/10.1016/j.marpolbul.2019.06.012.

Schling, M., Compeán, R. G., Pazos, N., Bailey, A., Arkema, K., Ruckelshaus, M., 2022. The economic impact of Sargassum: Evidence from the Mexican coast. Inter-American Development Bank, available at: https://publications.iadb.org/publications/english/document/The-Economic-Impact-of-Sargassum--Evidence-from-the-Mexican-Coast.pdf [Accessed 15 Dec. 2024].

Sentinelsat, December 2023. Sentinelsat (command line interface and Python API documentation). https://sentinelsat.readthedocs.io/en/stable/#.

Shirah, G., Mitchell, H., 2015. Garbage Patch Visualization Experiment. NASA Goddard Space Flight Center, available at: https://svs.gsfc.nasa.gov/4174 [Accessed 15 Dec. 2024].

Uribe-Martínez, A., Berriel-Bueno, D., Chávez, V., Cuevas, E., Almeida, K. L., Fontes, J. V. H., van Tussenbroek, B. I., Mariño-Tapia, I., Liceaga-Correa, M. d. l. A., Ojeda, E., Castañeda-Ramírez, D. G., Silva, R., 2022. Multiscale distribution patterns of pelagic rafts of sargasso (*Sargassum spp.*) in the mexican caribbean (2014–2020). Frontiers in Marine Science 9, https://doi.org/10.3389/fmars.2022.920339.

Van Tussenbroek, B. I., Arana, H. A. H., Rodríguez-Martínez, R. E., Espinoza-Avalos, J., Canizales-Flores, H. M., González-Godoy, C. E., Barba-Santos, M. G., Vega-Zepeda, A., Collado-Vides, L., 2017. Severe impacts of brown tides caused by *Sargassum spp.* on near-shore caribbean seagrass communities. Marine Pollution Bulletin 122 (1–2), 272–281, https://doi.org/10.1016/j.marpolbul.2017.06.057.

Wang, M., Hu, C., 2016. Mapping and quantifying *Sargassum* distribution and coverage in the central west atlantic using modis observations. Remote Sensing of Environment 183, 350–367, https://doi.org/10.1016/j.rse.2016.04.019.

Wang, M., Hu, C., 2020. Automatic extraction of *Sargassum* features from sentinel-2 msi images. IEEE Transactions on Geoscience and Remote Sensing 59 (3), 2579–2597, https://doi.org/10.1109/TGRS.2020.3002219.

Wang, M., Hu, C., 2021. Satellite remote sensing of pelagic *Sargassum* macroalgae: The power of high resolution and deep learning. Remote Sensing of Environment 264, 112631, https://doi.org/10.1016/j.rse.2021.112631.

Wang, M., Hu, C., Barnes, B. B., Mitchum, G., Lapointe, B., Montoya, J. P., 2019. The great atlantic *Sargassum* belt. Science 365 (6448), 83–87, https://doi.org/10.1126/science.aaw7912.

This article accompanies the following material:
Dynamic map: 10.22201/igg.25940694e.2024.2.123.19